VOLUME 7, NUMBER 1, JANUARY 2007

NANO LETTERS

Hydrogen Sieving and Storage in Fullerene Intercalated Graphite

Agnieszka Kuc,[†] Lyuben Zhechkov,[†] Serguei Patchkovskii,[‡] Gotthard Seifert,[†] and Thomas Heine*,[†]

Technische Universität Dresden, Fachbereich Chemie, D-01062 Dresden, Germany, and Steacie Institute for Molecular Sciences, NRC Canada, Ottawa, Canada

Received August 13, 2006; Revised Manuscript Received November 8, 2006

ABSTRACT

The geometrical properties of recently synthesised C_{60} intercalated in graphite have been confirmed by density-functional-based computer simulations. The capability of this material to store molecular hydrogen by physisorption is evaluated. While the material can sieve H_2 from heavier molecular gases, our free energy calculations indicate that further tuning of the system by reducing the amount of intercalated fullerene cages is necessary to achieve H_2 loadings which are interesting for technical applications.

Nanoporous carbon structures are among the best candidates as hydrogen storage media for mobile applications.[1−5] Experiments in this field are very challenging.The well-known problems include the synthesis of well-defined materials, their characterization, passivation of surface area by gas impurities, and effects of the nanostructure's surface on the storage capacity.[1−3,6] We have recently studied the simplest atomistic model for slit pore aromatic carbon nanostructures and have shown that graphene sheets with well-defined interlayer distances might be good candidates as storage material for molecular hydrogen at moderate temperatures and pressures.[4] We have found that the capability of the material to store H_2 is determined by the interlayer distance c: at distances below $c = 5$ Å the H_2−graphene interaction potential was repulsive, and no H_2 can penetrate between the graphite layers. The maximum storage capacity was predicted for slit pore sizes slightly above $c \approx 6$ Å, in agreement with recent experimental results.[7] For larger interlayer distances, the capacity to store H_2 reduces continuously, and for the limit of a single graphene sheet ($c = \infty$), only insignificant uptake of H_2 on the layer surface was predicted. Our model calculations[4] showed that the optimum size of the slit pores is essential for achieving a reasonable hydrogen storage capacity. It remained to be discussed how graphene layers with well-defined interlayer distances can be produced.

It is thermodynamically impossible for H_2 to penetrate between the layers of graphite: According to the dispersion-corrected[8,9] (DC) density-functional-based tight-binding (DFTB) method[10,11] as implemented in the deMon code,[12] it requires 74 meV per carbon to increase the interlayer distance of graphite to ∼6 Å, that is, to the optimal distance where H_2 could penetrate into the material. Introduction of H_2 will restabilize the opened graphite layer, but only by about 125 meV per H_2. If all low-energy positions of the material

* Corresponding author. E-mail: thomas.heine@chemie.tu-dresden.de.
[†] Technische Universität Dresden, Fachbereich Chemie.
[‡] Steacie Institute for Molecular Sciences, NRC Canada.

10.1021/nl0619148 CCC: $37.00
Published on Web 12/06/2006

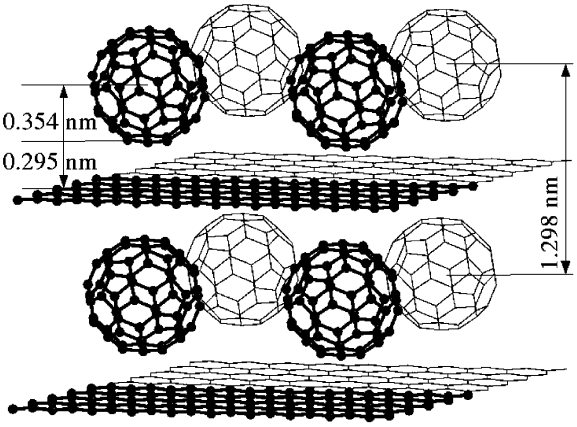

Figure 1. The extended unit cell of C_{60}-intercalated graphite. The fullerene cages form two-dimensional hexagonal layers.

are statically covered with H_2, six carbon atoms bind one hydrogen molecule.[13] In total, the penetration of H_2 into graphite is an endothermic process requiring at least 320 meV per H_2. Therefore, the interlayer distance of graphite needs to be increased by other means, and indeed, several possibilities have been discussed in the literature. They include functionalization of the sheets, for example by fluorination,[14,15] by doping with Li complexes,[16] or by oxidation with aquas acid agents, forming randomly spread out hydroxy and epoxide groups which increase the interlayer distance.[17,18] Functionalized graphite exhibits interlayer distances from 4.7 to 9 Å, depending on preparation and temperature. As functionalization transforms sp^2 carbon to sp^3, it allows covalent interlayer bonds and imposes loss of planarity.[19]

An alternative possibility to increase the interlayer distance while leaving the graphene sheets intact is the intercalation of spacer molecules. Thermodynamically, during the intercalation process, a destabilizing process—the interlayer van der Waals contacts are broken—is partially compensated by the formation of spacer-layer interactions. The intercalation of spacers into graphite is, however, possible: recently, the synthesis and characterization of graphite intercalated by C_{60} fullerenes has been reported.[20] The fullerene cages form a hexagonal two-dimensional lattice between the layers, and the transmission electron microscopy (TEM) image indicates that no covalent bonds between cages and graphene, neither between the fullerenes nor between them and the layers, are present.

The DC-DFTB optimized geometry of C_{60}-intercalated graphite (CIG) (Figure 1) agrees well with the reported TEM image of Gupta and co-workers.[20] In detail, the calculated interlayer distance is 12.985 Å and fits well the experimental value of 12.7 Å. The C_{60} radius is 3.542 Å at the DFTB level, in close agreement with 3.55 Å found in the X-ray experiment.[20] For the interlayer geometry, we used the experimentally observed hexagonal pattern with 12.5 Å lattice constant, which has been estimated from the TEM image of ref 20. We compare the stability of CIG with different carbon forms by means of atomization energies per carbon atom

$$E_{\text{atom}} = E_{\text{tot}}/N - E_{\text{free}}$$

Table 1. Calculated[9−12] Atomization Energies per C Atom (E_{atom}), Gap Energies (Δ), and Mass Densities (ρ) for Various Carbon Allotrops[a]

structure	E_{atom} (eV/atom)	Δ (eV)	ρ (g/cm^3)
graphite	−9.09	0 (0)[26]	2.27 (2.266)[26]
graphene layer	−8.90	0 (0)	
diamond	−8.87	6.88 (6.01)[26]	3.54 (3.514)[26]
C_{60} (gas phase)	−8.51	1.78 (1.7)	
C_{60} (solid)	−8.54	1.67 (1.70)[27]	1.73 (1.72)[27]
CIG	−8.71	0	1.28

[a] Experimental values are given in parentheses.

where E_{tot} denotes the total energy, N the number of carbon atoms in the nanostructure, and E_{free} the energy of a free carbon atom, with all energies calculated at the DC-DFTB level. CIG has an atomization energy per atom of −8.709 eV/atom. Hence, CIG is less stable than graphite (by 340 meV/atom) and more stable than C_{60} phases (by 170 meV/atom) (Table 1).

To assess the capability of CIG to host molecular hydrogen, we apply a method which we have recently proposed in ref 4: The interaction of H_2 with the carbon nanostructure is strongly influenced by the entropy of the system, and interaction free energies have to be calculated to assess the H_2 content of CIG. The free energy of the system can be calculated through statistical mechanics, for example, employing grand-canonical Monte Carlo simulations.[21−23] We chose a different, quantum mechanical route to assess the thermodynamics of the system: The partition function of the H_2 guest system is calculated quantum mechanically in one single simulation and allows the efficient evaluation of the entropy and interaction free energy: We solve the time-independent Schrödinger equation of a featureless particle with the mass of H_2 in the presence of the H_2−nanostructure interaction potential which is given on a grid. Repeating the same calculation for free H_2 gives the relative free energy with respect to the free gas, and other thermodynamic quantities are accessible. The interested reader is referred to ref 4, in particular to the Supporting Information of this article where validation and approximations of this methodology are discussed in detail. It should, however, be noted here that these values are those of ideal structures without contamination of the hydrogen phase with gas impurities.

We describe the H_2−CIG interaction employing a Lennard-Jones potential between all carbon atoms of the host structure and the H_2 center of mass. The potential has been parametrized earlier on the basis of post-Hartree−Fock ab initio calculations on the interaction of H_2 with polyaromatic hydrocarbons (PAHs).[4] The guest−host interaction is found to be attractive in the space between the fullerene cages and graphene and inside the fullerenes. As the interior of the fullerene cages will not contribute to the reversible H_2 storage capacity of the system, we put a repulsive value for the interaction potential on the grid points inside of the cages. The attractive part of the H_2-CIG interaction potential is given in Figure 2. As *active volume* we define the space of attractive H_2-host potential. For CIG the active volume is

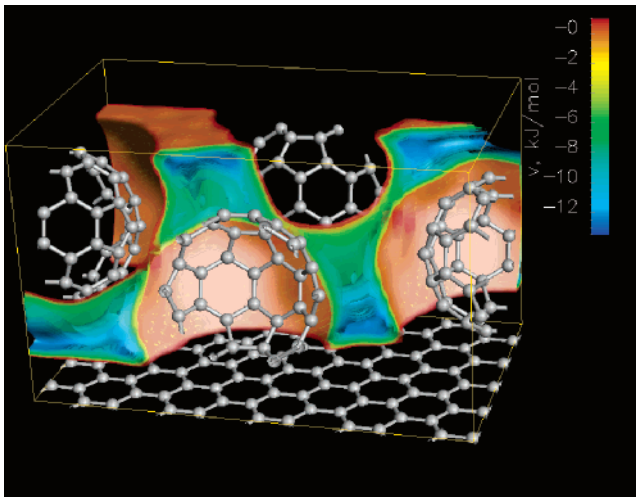

Figure 2. The interaction potential between H_2 and C_{60}-intercalated graphite (H_2-CIG). The figure shows potential energy isosurfaces in a diagonal cut through the unit cell.

found in the fosses and grooves between the fullerenes and the graphene sheets, where the potential reaches values of −12.5 kJ/mol. On the contrary, at the points of closest fullerene−fullerene and fullerene−graphene distance the H_2-host potential becomes repulsive. The active volume of CIG has been determined by numerical integration and is found to be 19% of the total volume. In comparison, the same structure without fullerene spacers has an active volume of 62%.

In Figure 3a we compare the interaction free energy of CIG with hypothetical graphite with the same interlayer distance as function of the temperature. Over the range of 50 K to ambient temperature, the spacers double the interaction free energy of CIG with H_2 compared to the empty structure. However, the supporting effect for H_2 storage due to lower free energy is partially compensated by the reduction of active volume, which is now taken by the fullerene cages. The resulting relative storage capacity, compared with free H_2 gas at same temperature and pressure, is given by the equilibrium constant (Figure 3b). The storage capacity might become interesting for practical applications at low temperatures and at moderate pressures (e.g., at 10 MPa and 200 K), Table 2. The density of H_2 states (density-of-states, DOS) in CIG is given in Figure 4. It shows

Table 2. Hydrogen Storage Capacities of Selected Materials[a]

material	T (K)	P_{ext} (MPa)	gw (%)	V_c (g/cm^3)
CNT	298−773	0.1	0.4 (0.3/0.7)[b]	0.0032
Li-doped CNT	473−673	0.1	20.0	0.180
Li-doped graphite	473−673	0.1	14.0	0.280
K-doped CNT	<313	0.1	14.0	0.0126
K-doped graphite	<313	0.1	5.0	0.060
FeTi−H	>263	2.5	<2	0.096
NiMg−H	>523	2.5	<4	0.081
cryoadsorption	∼77	20	∼5	0.020
isooctane/gasoline	>233	0.1	17.3	0.117
CIG	300	10	(3.5)	(0.060)
	250	10	(5.7)	(0.071)
	200	10	(9.1)	(0.120)

[a] The strorage temperature (T), external pressure (P_{ext}), gravimetric density (gw), and volumetric density (V_c) are compared. Experimental values are taken from ref 28, while those calculated for this work are given in parentheses. [b] Model calculations of a carbon nanotube with chirality (6,6) and ∼7 Å diameter at ambient conditions give gravimetric storage capacities of 0.3% in the interior of a CNT and 0.7% in a bundle.

that C_{60} spacers lower the energy levels populated by H_2, but they reduce the total amount of available binding states compared to hypothetical graphite with the same interlayer distance. Comparison with the low H_2 storage capacity of carbon nanotube ropes indicates the importance of the topology of the nanostructure: CIG is a solid which does not suffer as strongly from surface effects as CNT bundles.[24] In CIG, the inactive volume in the interior of the fullerenes is smaller than that inside the CNTs. Moreover, due to graphene layers CIG is less affected by the fact that the concave outer walls of CNTs and fullerenes are less attractive to H_2.[25]

Further, we calculated the diffusion coefficients of H_2 and N_2 inside CIG using Born−Oppenheimer molecular dynamics simulations, employing the DC-DFTB method using a NVE ensemble at 300 K for 1 ns. The H_2 diffusion constant is calculated to be $\sim 8.5 \times 10^{-3}$ cm^2/s, while the values for the other molecules are more than 1 order of magnitude lower (3.8×10^{-4} cm^2/s for N_2 and 1.7×10^{-4} cm^2/s for C_{60} itself). These values show that N_2 is trapped between the C_{60} molecules, while H_2 can easily penetrate through the structure and move between the bucky balls and the graphene layers.

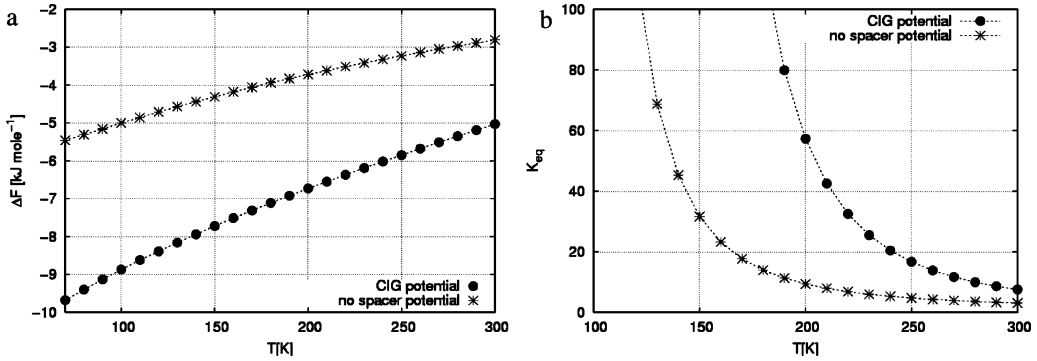

Figure 3. The dependence of free energy (a) and equilibrium constant (b) with respect to the temperature, within the ideal gas approximation for H_2. Values for C_{60}-intercalated graphite (circles) are compared with those of hypothetical graphite with the same interlayer distance (crosses).

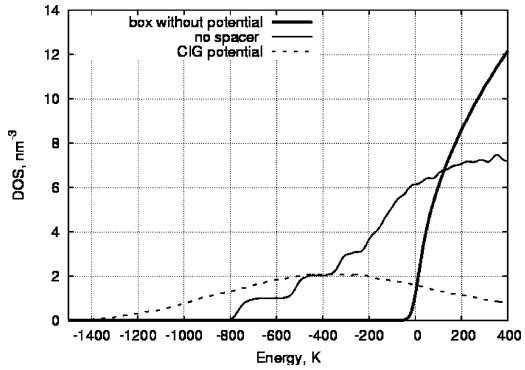

Figure 4. Density of states (DOS) of molecular hydrogen in C_{60}-intercalated graphite, hypothetical graphite with same interlayer distance and of a potential-free simulation box.

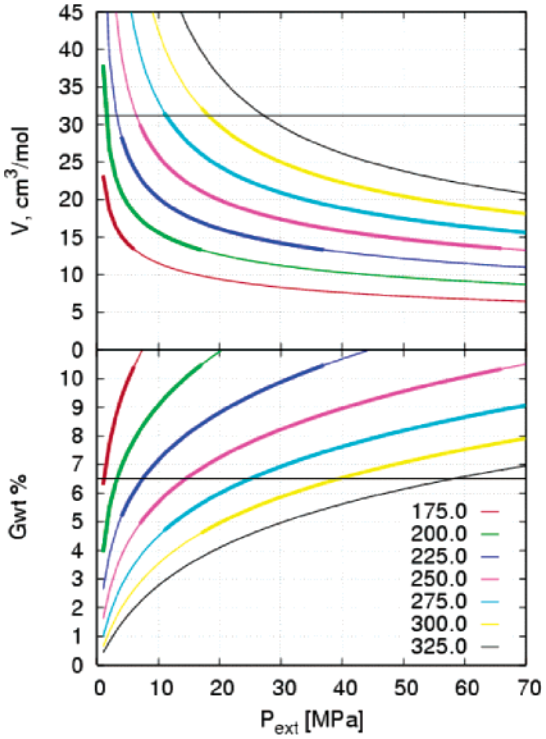

Figure 5. Volumetric (top) and gravimetric storage capacities of CIG, calculated from the real gas equation of state, as function of the external pressure are given for various temperatures (color coded). For bold lines, our approximations are on safe grounds. The targets of the Department of Energy of the USA for automotive applications (Gwt = 6.5%, V = 31.2 cm^3/mol) are indicated as horizontal lines.

In conclusion, our simulations confirm the structure of the recently reported C_{60} intercalated graphite, and the stability of the material is in the expected range.[20] Experiment and simulation agree very closely on the geometrical parameters. The electronic properties of CIG are similar to those of graphite. We showed that intercalation of graphite by fullerenes is an interesting way to follow for realization of H_2 storage devices based on physisorption in carbon nanostructures. The shape of the spacers allows a nearly free penetration of H_2 into and out of the material with no effect on its structural and mechanical properties. The spacers double the interaction free energy of the material with H_2 in the limit of the low hydrogen gas pressure. On the other hand, the fullerenes reduce the active volume of 62% of the structure without spacers to 19% in CIG in the case of closest packed hexagonal cage. Gravimetric and volumetric storage capacities of H_2 in CIG are given in Figure 5. Compared to other candidate systems for hydrogen storage, CIG approaches values obtained for Li-doped carbon systems at low temperatures (Table 2). As H_2 is only physisorbed in CIG has, however, the advantage of easy loading and unloading over metal hydrides and alkali-doped carbon structures. The storage capacity might become interesting for practical applications at low temperatures and at moderate pressures (e.g., at 10 MPa and 200 K). An even more promising material for the storage of molecular hydrogen could be created if it would be possible to reduce the density of C_{60} inside CIG. However, CIG may prove a useful part of a composite storage system, by providing in situ separation of H_2 from other gases contained in air by molecular sieving.

Acknowledgment. Financial support of Energiestiftung Baden-Württemberg and of the Deutsche Forschungsgemeinschaft is acknowledged. Computer simulations have been carried out partially at ZIH Dresden.

References

(1) Liu, C.; Cheng, H. M. Carbon nanotubes for clean energy applications. *J. Phys. D: Appl. Phys.* **2005**, *38* (14), R231−R252.
(2) Eletskii, A. V. Sorption properties of carbon nanostructures. *Phys.−Usp.* **2004**, *47*, 1119−1154.
(3) Strobel, R.; Garche, J.; Moseley, P. T.; Jorissen, L.; Wolf, G. Hydrogen storage by carbon materials. *J. Power Sources* **2006**, *159* (2), 781−801.
(4) Patchkovskii, S.; Tse, J. S.; Yurchenko, S. N.; Zhechkov, L.; Heine, T.; Seifert, G. Graphene nanostructures as tunable storage media for molecular hydrogen. *Proc. Natl. Acad. Sci. U.S.A.* **2005**, *102* (30), 10439−10444.
(5) Terres, E.; Panella, B.; Hayashi, T.; Kim, Y. A.; Endo, M.; Dominguez, J. M.; Hirscher, M.; Terrones, H.; Terrones, M. Hydrogen storage in spherical nanoporous carbons. *Chem. Phys. Lett.* **2005**, *403* (4−6), 363−366.
(6) Zhechkov, L.; Heine, T.; Seifert, G. Physisorption of N-2 on graphene platelets: An ab initio study. *Int. J. Quantum Chem.* **2006**, *106* (6), 1375−1382.
(7) Gogotsi, Y.; Dash, R. K.; Yushin, G.; Yildirim, T.; Laudisio, G.; Fischer, J. E. Tailoring of nanoscale porosity in carbide-derived carbons for hydrogen storage. *J. Am. Chem. Soc.* **2005**, *127* (46), 16006−16007.
(8) Elstner, M.; Hobza, P.; Frauenheim, T.; Suhai, S.; Kaxiras, E. Hydrogen bonding and stacking interactions of nucleic acid base pairs: A density-functional-theory based treatment. *J. Chem. Phys.* **2001**, *114* (12), 5149−5155.
(9) Zhechkov, L.; Heine, T.; Patchkovskii, S.; Seifert, G.; Duarte, H. A. An efficient a Posteriori treatment for dispersion interaction in density-functional-based tight binding. *J. Chem. Theory Comput.* **2005**, *1* (5), 841−847.
(10) Porezag, D.; Frauenheim, T.; Kohler, T.; Seifert, G.; Kaschner, R. Construction of Tight-Binding-Like Potentials on the Basis of Density-Functional Theory - Application to Carbon. *Phys. Rev. B* **1995**, *51* (19), 12947−12957.
(11) Seifert, G.; Porezag, D.; Frauenheim, T. Calculations of molecules, clusters, and solids with a simplified LCAO-DFT-LDA scheme. *Int. J. Quantum Chem.* **1996**, *58* (2), 185−192.
(12) Köster, A. M.; Geudtner, G.; Goursot, A.; Heine, T.; Vela, A.; Patchkovskii, S.; Salahub, D. R. *deMon 2003 1.1*; NRC: Canada, 2004.
(13) Heine, T.; Zhechkov, L.; Seifert, G. Hydrogen storage by physisorption on nanostructured graphite platelets. *Phys. Chem. Chem. Phys.* **2004**, *6* (5), 980−984.
(14) Guerin, K.; Pinheiro, J. P.; Dubois, M.; Fawal, Z.; Masin, F.; Yazami, R.; Hamwi, A. Synthesis and characterization of highly fluorinated graphite containing sp(2) and sp(3) carbon. *Chem. Mater.* **2004**, *16* (9), 1786−1792.

(15) Gupta, V.; Nakajima, T.; Ohzawa, Y.; Zemva, B. A study on the formation mechanism of graphite fluorides by Raman spectroscopy. *J. Fluorine Chem.* **2003**, *120* (2), 143−150.
(16) Deng, W. Q.; Xu, X.; Goddard, W. A. New alkali doped pillared carbon materials designed to achieve practical reversible hydrogen storage for transportation. *Phys. Rev. Lett.* **2004**, *92* (16), 166103.
(17) He, H. Y.; Klinowski, J.; Forster, M.; Lerf, A. A new structural model for graphite oxide. *Chem. Phys. Lett.* **1998**, *287* (1−2), 53−56.
(18) Lerf, A.; He, H. Y.; Forster, M.; Klinowski, J. Structure of graphite oxide revisited. *J. Phys. Chem. B* **1998**, *102* (23), 4477−4482.
(19) Telling, R. H.; Ewels, C. P.; El-Barbary, A. A.; Heggie, M. I. Wigner defects bridge the graphite gap. *Nat. Mater.* **2003**, *2* (5), 333−337.
(20) Gupta, V.; Scharff, P.; Risch, K.; Romanus, H.; Muller, R. Synthesis of C-60 intercalated graphite. *Solid State Commun.* **2004**, *131* (3−4), 153−155.
(21) Deng, W. Q.; Xu, X.; Goddard, W. A. New alkali doped pillared carbon materials designed to achieve practical reversible hydrogen storage for transportation. *Phys. Rev. Lett.* **2004**, *92* (16) 166103.
(22) Wang, Q. U.; Johnson, J. K.; Broughton, J. Q. Thermodynamic properties and phase equilibrium of fluid hydrogen from path integral simulations. *Mol. Phys.* **1996**, *89* (4), 1105−1119.
(23) Marx, D.; Nielaba, P. Path-Integral Monte-Carlo Techniques For Rotational Motion In 2 Dimensions—Quenched, Annealed, And No-Spin Quantum-Statistical Averages. *Phys. Rev. A* **1992**, *45* (12), 8968−8971.
(24) Williams, K. A.; Eklund, P. C. Monte Carlo simulations of H-2 physisorption in finite-diameter carbon nanotube ropes. *Chem. Phys. Lett.* **2000**, *320* (3−4), 352−358.
(25) Okamoto, Y.; Miyamoto, Y. Ab initio investigation of physisorption of molecular hydrogen on planar and curved graphenes. *J. Phys. Chem. B* **2001**, *105* (17), 3470−3474.
(26) Greenwood, N. N.; Earnshaw, A. *Chemistry of the elements*; Elsevier: Amsterdam, 1997.
(27) Dresselhaus, M. S.; Dresselhaus, G. Fullerenes And Fullerene-Derived Solids As Electronic Materials. *Annu. Rev. Mater. Sci.* **1995**, *25*, 487−523.
(28) Chen, P.; Wu, X.; Lin, J.; Tan, K. L. High H-2 uptake by alkali-doped carbon nanotubes under ambient pressure and moderate temperatures. *Science* **1999**, *285* (5424), 91−93.

NL0619148